

On the Dynamical Overstability of Radiative Blast Waves: The Atomic Physics of Shock Stability

J. Martin Laming*

*Space Science Division Code 7674L,
Naval Research Laboratory, Washington DC 20375*

Jacob Grun†

*Plasma Physics Division Code 6795,
Naval Research Laboratory, Washington DC 20375*

(Dated: November 2, 2018)

Abstract

Atomic physics calculations of radiative cooling are used to calculate criteria for the overstability of radiating shocks. Our calculations explain the measurement of shock overstability by Grun et al. and explain why the overstability was not observed in other experiments. The methodology described here can be especially useful in astrophysical situations where the relevant properties leading to an overstability can be measured spectroscopically, but the effective adiabatic index is harder to determine.

PACS numbers: 52.30.-q, 52.35.Tc, 52.50.Lp, 52.72.+v

*Electronic address: jlaming@ssd5.nrl.navy.mil

†Electronic address: grun@nrl.navy.mil

Shocks play a crucial role in the death and rebirth of stars. At the endpoint of stellar evolution, a supernova explosion launches a blast wave out into the surrounding medium with a velocity in the range 10,000 - 20,000 km s⁻¹. After about 10,000 years the blast wave slows to speeds of order 200 km sec⁻¹ and becomes “radiative”, i.e. radiative energy losses from a “cooling zone” some distance behind the shock front itself become an important consideration in the overall shock dynamics. Radiative shocks are subject to a number of interesting hydrodynamic instabilities and oscillations. A velocity dependent cooling instability may develop as the shock slows [1, 2, 3, 4]. This causes large amplitude fluctuations in the shock velocity and in the distance between the shock front and the radiative cooling zone. When the shock slows sufficiently that the cooling instability dies away, and the distance between the shock front and the cooling zone is much smaller, it can become subject to a new instability, an oscillatory rippling of its front that grows as a power of time [5, 6, 7, 8, 9]. The ripples grow because the thermal pressure of the shocked gas, which is perpendicular to the local shock front, is not necessarily parallel to the ram pressure of the upstream plasma, which is directed along the shock velocity vector. In shocks with sufficiently high compression this imbalance of pressures induces oscillatory movement of material within the shock shell. Parts of the shell that contain less mass slow down more than the parts of the shell that contain more mass and a growing oscillation ensues. In its nonlinear phase [7] knots or clumps of material may form with sizes similar to the shocked shell thickness. It is possible that local nonuniformities in interstellar gas caused by the aforementioned instabilities provide the initial conditions for gravitational collapse and the subsequent birth of new stars.

The existence of growing ripples in radiative shock fronts was demonstrated in a laboratory experiment by Grun et al. [10]. These authors produced blast waves in nitrogen and xenon gas and showed that shocks in the more radiative xenon gas rippled with a power-law growth rate close to theoretical predictions, whereas shocks in nitrogen remained stable. More recently other researchers, working in a somewhat different parameter space, attempted to produce the rippling overstability, but were unable to do so [11].

In this paper we perform detailed calculations of the radiative cooling of a shock front in nitrogen and xenon plasma from which we derive the effective adiabatic index γ_{eff} and using [6] infer the growth rate of the overstability, with the aim of understanding just how radiative a radiative shock needs to be to be overstable. We find that in practice in the

laboratory examples we consider, the shocked plasma must cool significantly during the shock transition, which is a distance of order the ion mean free path [12, 13]. We compare our results to experiments [10, 11] and show why [10] were able to observe the overstability and why [11] could not. Since determining γ_{eff} from cooling calculations is dependent on quantities such as element abundances, densities, temperatures and shock velocities that can be measured spectroscopically, the formalism we present can be helpful in astrophysical situations where the effective adiabatic index is otherwise much harder to determine.

Our method for computing the radiative cooling follows that in [14]. The Coulomb logarithm is set to its appropriate value, and three body recombination is included, as is appropriate for high density plasma. For N, we use collisional ionization and radiative and dielectronic recombination rates from [15]. Ionization cross sections for Xe^{2-6+} and Xe^{8+} can be found in [16, 17, 18, 19, 20], from which rates were calculated and fitted to a Lotz formula. Rates for Xe, Xe^+ and Xe^{7+} were estimated by interpolation and extrapolation. We are unaware of recombination rates for these Xe ions, so for radiative and dielectronic recombination we substituted the corresponding rates for Ar from [15]. This should not lead to large errors, since the ground configurations of Xe and Ar are $5s^25p^6$ and $3s^23p^6$ respectively, and in most of the blast waves we model, Xe does not ionize into the $4d^{10}$ subshell. In any case three body recombination is usually dominant. Radiative cooling rates for N II and N III are calculated from collisional data given in [21, 22] and radiative data from [23, 24, 25] and the Opacity Project. Cooling rates for more highly charged ions of N and for the Xe ions were computed using the HULLAC suite of codes [26, 27]. All cooling rates were tabulated at a nominal electron density of $n_e = 10^{17} \text{ cm}^{-3}$, and fitted to formulae of the form $(1 + a(n_e/10^{17} - 1))^{-1}$ where a is a constant for each ion to model the density dependence. We neglect the small temperature dependence of a . The rates for N and Xe at $n_e = 10^{17} \text{ cm}^{-3}$ were similar to those tabulated in [28] for N (interpolated from those for C and O) and for Ar. The cooling rate for Xe X, the most highly charged Xe ion in our model is the same as Ar X in [28] multiplied by a factor of 10, obtained by comparison with results in [29].

Another modification made to [14] is the use of a more realistic density profile for the expanding laser target, though this makes little difference to the blast wave evolution in the Sedov-Taylor phase. With the appropriate ambient gas density and a nominal ablated target kinetic energy of 100 or 200 J for N or Xe respectively (coming from the energy of the laser

pulse [10]) we calculate the blast wave velocity and radius as a function of time after the laser pulse. At each time we compute a steady state radiative shock structure, demanding that the photoionizing radiation produced by the shocked gas must produce a self-consistent preshock ionization state. Photoionization rates are taken from [30], with those for Ar substituting for Xe. For neutral Xe at least, the photoionization cross section is very similar to that for neutral Ar [31, 32]. We assumed the radiative cooling in neutral N or Xe was ineffective due to opacity, and the temperature of the preshock gas (the shock precursor) is calculated by balancing the heating by photoionization with radiative cooling. We also checked that molecular N_2 was completely dissociated in the precursor by the radiation field using photoionization/dissociation cross sections compiled at <http://www.space.swri.edu/amop/>, dissociative recombination [33], electron impact dissociation [34, 35] and recombination [36]. In any case our precursor temperatures are generally sufficiently high that N_2 dissociation should not be an issue.

We model the shock interior by setting electron and ion temperatures equal to the values given by the jump conditions added to their preshock temperatures. We then follow a Lagrangian plasma element through the shock by integrating the simultaneous equations for the ionization balance and electron and ion temperatures accounting for electron-ion collisional equilibration, radiation and ionization energy losses. After each time step we modify particle temperatures and number densities according to the effects of adiabatic expansion of the blast wave, and radiative and ionization losses in an assumed constant pressure environment. We proceed in this manner for a time 400 ns following the laser pulse. Once the Lagrangian element has moved a distance d , the shock width, given by [12, 13] $d = \langle (4/3) 2\gamma / (\gamma + 1) v_i \tau_{ii} \rangle$ we evaluate γ at each time step from the density enhancement of the plasma element relative to the preshock value. In the expression for d , v_i and τ_{ii} are the ion thermal speed and self collision time respectively and the angled brackets $\langle \dots \rangle$ denote a time average through the shock transition.

The evolution of the electron and ion temperatures with distance behind the shock onset are plotted in Figure 1 for the Xe blast wave 120 ns after the laser pulse, and the corresponding evolution of the ionization balance is given in Figure 2. We evaluate an average γ_{eff} for various times in the evolution of the blast wave from the average density enhancement in the accumulated shell of shocked gas over the preshock density. These values are given in Tables I for N and II for Xe. We also give at each time t the shock velocity v_s , radius R ,

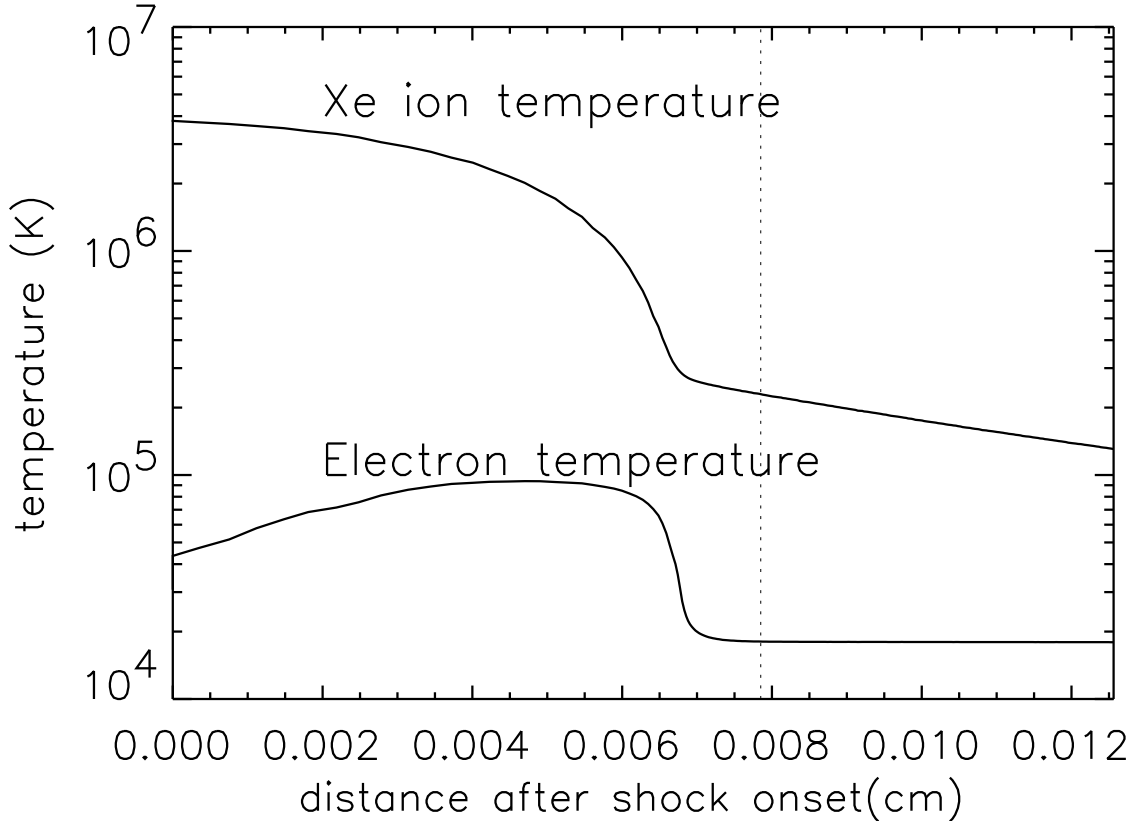


FIG. 1: The spatial evolution of the electron and Xe ion temperatures behind the shock front at 120 ns after laser pulse. Distance is measured from the shock onset. The width of the shock is 7.85×10^{-3} cm, indicated by the vertical dotted line.

the initial ionization state and temperature T , and the Mach number M appropriate to the precursor temperature T .

We evaluate the growth exponent $\text{real}(s)$ and the value of $l = kR$ for each blast wave from equations 19 in [6]. The maximum $\text{real}(s)$ and the l at which this occurs are given in the penultimate two columns of Tables I and II. In this calculation we take the shell thickness as a fraction of the blast wave radius to be $H/R = (\gamma_{\text{eff}} - 1) / (\gamma_{\text{eff}} + 1) / 3$. The ranges of $\text{real}(s)$ and l given in the tables correspond to taking $R \propto t^m$ with $m = 2/5$ for adiabatic Sedov-Taylor behavior or $m = 2/7$ for the strongly radiating pressure driven snowplow case, which gives the higher values of $\text{real}(s)$ and l . This is expected to be the case for the blast wave under consideration, although the data of [10] appear to be slightly more consistent

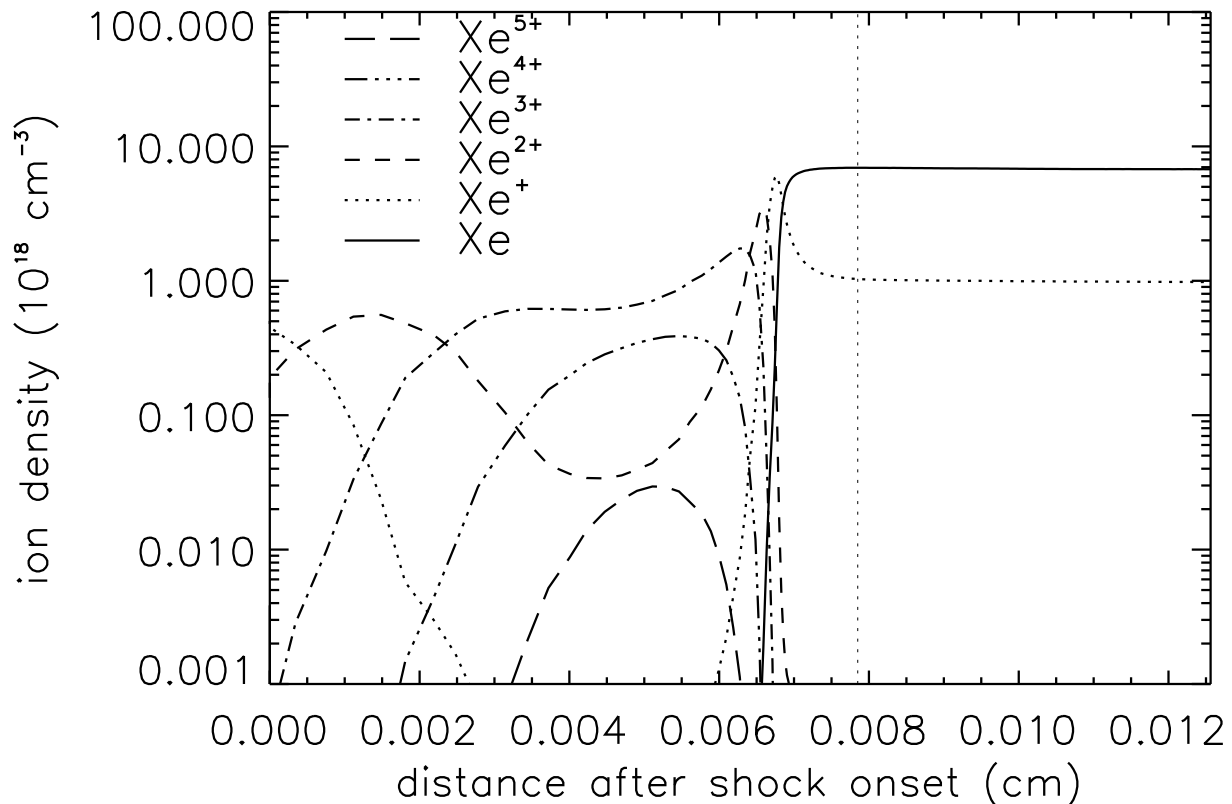


FIG. 2: The spatial evolution of the Xe ionization balance at 120 ns after the laser pulse.

with $m = 2/5$. However if the energy radiated by the shocked plasma is absorbed upstream and consequently swept back up by the shock, [11] speculate that behavior closer to the Sedov-Taylor limit may be observed even for strongly radiating shocks, and this limit was assumed in the calculations of ionization balance and radiative cooling. Examples of the stability calculations are given in Figure 3 for Xe at 60 ns, 120 ns, and 240 ns, which follow the transition from strong overstability through to stability for $m = 2/7$. We find generally that γ_{eff} must be closer to 1 for overstability than in the original work [5]. This is because we calculate the Mach number independently of γ_{eff} whereas [5] couple them to ensure an isothermal shock, as in equation (22) of [6]. The final column in Tables I and II gives the fraction of the kinetic energy of the incident upstream plasma (in the shock rest frame) that is radiated away during the shock transition, ϵ . This is estimated by identifying the γ we calculate at distance d behind the shock with the γ_1 parameter in [37, 38], and using their

TABLE I: Model parameters for N blast wave, 100 J laser pulse.

t	v_s	R	N	N ⁺	N ²⁺	T	M	γ_{eff}	real(s_{max})	l_{max}	ϵ
(ns)	(km s ⁻¹)	(cm)				(K)					
40	87.5	0.68	0.109	0.845	0.046	32200	15.6	1.045	-0.016→0.32	82→114	0.89
80	58.7	0.96	0.211	0.776	0.013	30100	10.8	1.20	-0.25→ -0.065		0.49
120	44.1	1.16	0.377	0.621	0.002	28100	8.3	1.26			0.23
160	36.3	1.32	0.538	0.462	0.001	26200	7.1	1.23			0.17
200	31.4	1.45	0.684	0.316	0.0	24800	6.3	1.22			0.14

TABLE II: Model parameters for Xe blast wave, 200 J laser pulse.

t	v_s	R	Xe	Xe ⁺	Xe ²⁺	Xe ³⁺	Xe ⁴⁺	T	M	γ_{eff}	real(s_{max})	l_{max}	ϵ
(ns)	(km s ⁻¹)	(cm)						(K)					
40	75.3	0.60	0.0	0.040	0.652	0.281	0.027	46100	34.2	1.19			0.596
60	57.3	0.73	0.0	0.263	0.718	0.019	0.0	37400	28.9	1.015	0.60→0.86	257→349	0.963
80	47.0	0.84	0.001	0.439	0.554	0.006	0.0	35100	24.5	1.025	0.13→0.45	152→210	0.942
100	40.5	0.93	0.003	0.647	0.349	0.001	0.0	32600	21.9	1.028	0.13→0.45	135→187	0.918
120	36.0	1.00	0.006	0.784	0.210	0.0	0.0	30700	20.0	1.033	0.046→0.38	114→158	0.901
160	29.9	1.13	0.019	0.917	0.065	0.0	0.0	27700	17.5	1.048	-0.17→0.19	77→108	0.876
200	26.0	1.24	0.047	0.935	0.018	0.0	0.0	25100	16.0	1.057	-0.23→ 0.13	64→91	0.851
240	23.2	1.34	0.101	0.894	0.005	0.0	0.0	23100	14.9	1.075	-0.253→0.021	< 69	0.825
300	20.2	1.47	0.207	0.792	0.001	0.0	0.0	19000	13.5	1.096	< -0.044		0.775
400	16.9	1.66	0.406	0.594	0.0	0.0	0.0	19000	12.0	1.13	< -0.067		0.710

relation between ϵ and γ_1 .

From Tables I and II, our results are in qualitative agreement with the observations in [10]. The N blast wave is stable at all times (except at 40 ns, but here the blast wave evolution is probably still dominated by the exploding target) whereas the Xe blast wave shows overstability for times between 60 and 150-300 ns, depending on the value of m . The predicted stabilization for Xe at 150 - 300 ns is in good agreement with observations. However we still predict growth at lower s and higher l than actually observed, though

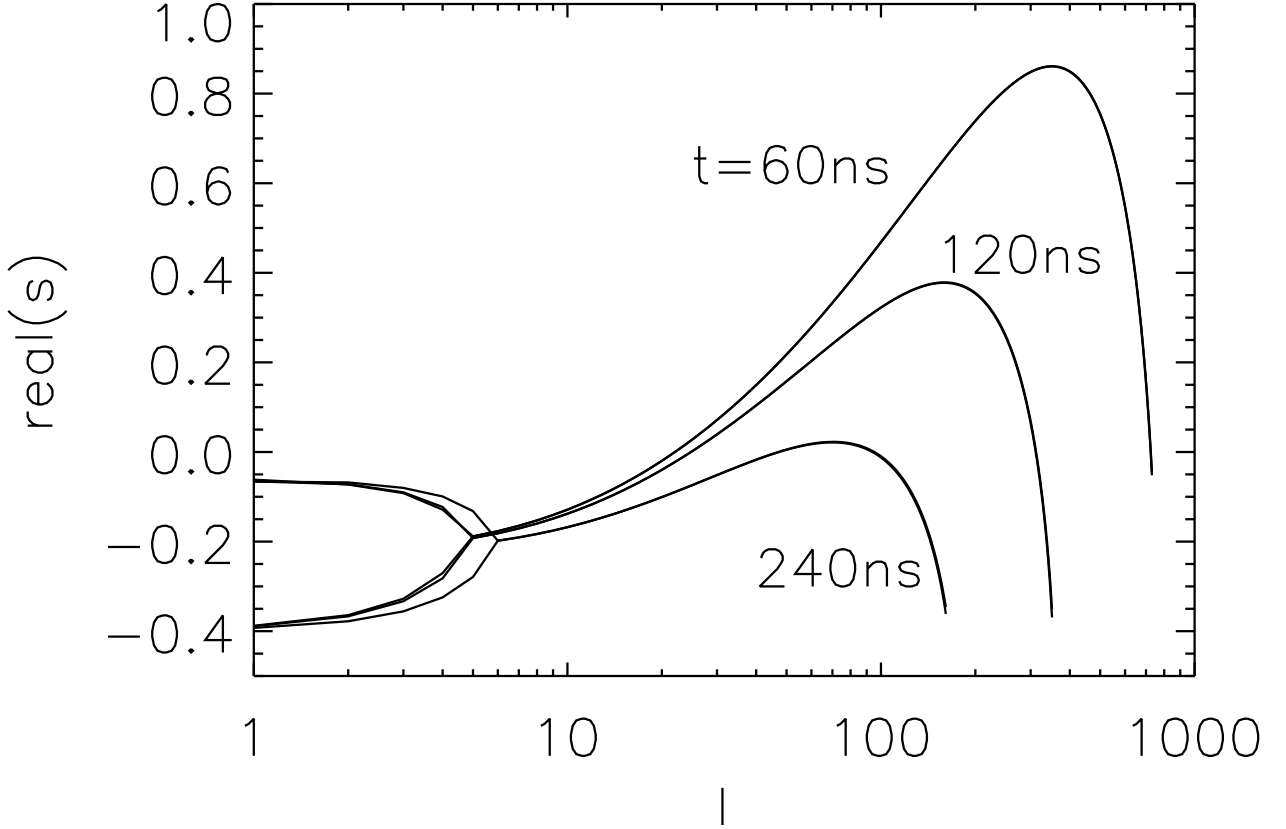


FIG. 3: Plots of $\text{real}(s)$ where the overstability grows as t^s , for Xe blast waves observed at 60, 120, and 240 ns after the laser pulse. Curves are calculated from equations 19 of reference [6], using shock parameters given in Table II.

[10] caution that their measurements of kR may not be identical to the l in the theory. Additionally the theory only treats the linear regime, while the measurements presumably include non-linear effects.

The overstability is suppressed at early times because insufficient time has elapsed to allow the shock heated Xe plasma to cool significantly. Similar speed blast waves launched by a more energetic laser pulse (and thus having decelerated from a higher initial velocity with more time available for cooling) would be overstable. At late times the blast wave stabilizes simply because the radiative power loss becomes insufficient at the lower shock speeds. From Table II it appears that approximately 80-90% of the incident plasma kinetic energy must be radiated in the shock transition before overstability occurs. It is also now

clear why overstabilities were not observed in [11]. They launched shocks in Xe gas at atmospheric pressure with velocities initially 15 km s^{-1} slowing to around 6 km s^{-1} . The blast waves in [10] were initiated at speeds of order 100 km s^{-1} in Xe gas at 5 torr pressure. From Table II it is clear that at 5 torr pressure below a minimum shock speed of around 25 km s^{-1} Xe will no longer be overstable. This minimum shock speed will likely be higher for Xe shocks at atmospheric pressure, since the higher density will reduce radiative cooling rate by electron collisional depopulation of excited levels.

We believe that we have captured the essential physics of the radiative blast waves observed in [10]. A more rigorous treatment must dispense with the fluid approximation and use a kinetic theory description of the plasma. However such a calculation with the necessary atomic physics is probably some years away in terms of the computing resources required. The fundamental reason why the N blast waves are stable is not so much that N is inherently less radiative than Xe at the relevant temperatures, but that its radiation is more suppressed in our cooling calculations by the electron density than that for Xe. However we do still expect that heavy element plasmas, rather than the H-He dominated cosmic composition, will be more susceptible to the overstability. Thus a promising astrophysical environment in which to look for such effects might be the heavy element rich plasma in the ejecta of supernova remnants, for which the reverse shock can be radiative in early phases [39].

Acknowledgments

We acknowledge support by basic research funds of the Office of Naval Research (JML), as well as support from NRL 6.2 Award N0001402WX30007 and ONR Award N0001402WX20803 (JG). We thank Dr Judah Goldwasser from ONR for his support and encouragement.

-
- [1] R. A. Chevalier and J. N. Imamura, *Astrophys. J.* **261**, 543 (1982).
 - [2] D. E. Innes, J. R. Gidding, and S. A. E. G. Falle, *Mon. Not. R. Astron. Soc.* **226**, 67 (1987).
 - [3] T. J. Gaetz, R. J. Edgar, and R. A. Chevalier, *Astrophys. J.* **329**, 927 (1988).
 - [4] P. A. Kimoto and D. F. Chernoff, *Astrophys. J.* **485**, 274 (1997).
 - [5] E. T. Vishniac, *Astrophys. J.* **274**, 152 (1983).

- [6] E. T. Vishniac and D. Ryu, *Astrophys. J.* **337**, 917 (1989).
- [7] M.-M. M. Low and M. L. Norman, *Astrophys. J.* **407**, 207 (1993).
- [8] D. Ryu and E. T. Vishniac, *Astrophys. J.* **313**, 820 (1987).
- [9] E. Bertschinger, *Astrophys. J.* **304**, 154 (1986).
- [10] J. Grun, J. Stamper, C. Manka, J. Resnick, R. Burris, J. Crawford, and B. H. Ripin, *Phys. Rev. Lett.* **66**, 2738 (1991).
- [11] M. J. Edwards, A. J. MacKinnon, J. Zweiback, K. Shigemori, D. Ryutov, A. M. Rubenchik, K. A. Keilty, E. Liang, B. A. Remington, and T. Ditmire, *Phys. Rev. Lett.* **87**, 085004 (2001).
- [12] L. D. Landau and E. M. Lifshitz, *Fluid Mechanics 2nd edition* (Pergamon, 1987).
- [13] M. A. Liberman and A. L. Velikovich, *The Physics of Shock Waves in Gases and Plasmas* (Springer-Verlag, 1986).
- [14] J. M. Laming, *Astrophys. J.* **563**, 828 (2001).
- [15] P. Mazzotta, G. Mazzitelli, S. Colafrancesco, and N. Vittorio, *Astron. Astrophys. Supp. Ser.* **133**, 403 (1998).
- [16] D. C. Griffin, C. Bottcher, M. S. Pindzola, S. M. Younger, D. C. Gregory, and D. H. Crandall, *Phys. Rev. A* **29**, 1729 (1984).
- [17] D. C. Gregory, P. F. Dittner, and D. H. Crandall, *Phys. Rev. A* **27**, 724 (1983).
- [18] D. C. Gregory and D. H. Crandall, *Phys. Rev. A* **27**, 2338 (1983).
- [19] M. E. Bannister, D. E. Mueller, L. J. Wang, M. S. Pindzola, D. C. Griffin, and D. C. Gregory, *Phys. Rev. A* **38**, 38 (1988).
- [20] K. F. Man, A. C. H. Smith, and M. F. A. Harrison, *J. Phys. B* **26**, 1365 (1993).
- [21] R. P. Stafford, K. L. Bell, A. Hibbert, and W. P. Wijesundera, *Mon. Not. R. Astron. Soc.* **268**, 816 (1994).
- [22] R. P. Stafford, K. L. Bell, and A. Hibbert, *Mon. Not. R. Astron. Soc.* **266**, 715 (1994).
- [23] M. E. Galavis, C. Mendoza, and C. J. Zeippen, *Astron. Astrophys. Supp. Ser.* **123**, 159 (1997).
- [24] C. Mendoza, C. J. Zeippen, and P. J. Storey, *Astron. Astrophys. Supp. Ser.* **135**, 159 (1999).
- [25] H. Nussbaumer and P. J. Storey, *Astron. Astrophys.* **71**, L5 (1979).
- [26] A. Bar-Shalom and M. Klapisch, *Comput. Phys. Commun.* **50**, 375 (1988).
- [27] A. Bar-Shalom, M. Klapsich, and J. Oreg, *Phys. Rev. A* **38**, 1773 (1988).
- [28] H. P. Summers and R. W. P. McWhirter, *J. Phys. B* **12**, 2387 (1978).
- [29] D. E. Post, R. V. Jensen, C. B. Tarter, W. H. Grasberger, and W. A. Lokke, *Atomic Data*

- and Nuclear Data Tables **20**, 397 (1977).
- [30] D. A. Verner, G. J. Ferland, K. T. Korista, and D. G. Yakovlev, *Astrophys. J.* **465**, 487 (1996).
 - [31] C. T. Chantler, *J. Phys. Chem. Ref. Data* **24**, 71 (1995).
 - [32] B. L. Henke, J. C. Davis, E. C. Gullikson, and R. C. C. Perera, Lawrence Berkely Laboratory Report LBL-26259 UC-411 (1988).
 - [33] D. Kella, P. J. Johnson, H. B. Pedersen, L. Vejby-Christensen, and L. H. Andersen, *Phys. Rev. Lett.* **77**, 2432 (1996).
 - [34] J. M. Ajello and M. Ciocca, *J. Geophys. Res.* **101**, 18953 (1996).
 - [35] D. T. Stibbe and J. Tennyson, *Astrophys. J.* **513**, L147 (1999).
 - [36] M. A. A. Clyne and D. H. Stedman, *J. Phys. Chem.* **71**, 3071 (1967).
 - [37] E. Cohen, T. Piran, and R. Sari, *Astrophys. J.* **509**, 717 (1998).
 - [38] E. Liang and K. Keilty, *Astrophys. J.* **533**, 890 (2000).
 - [39] R. A. Chevalier and C. Fransson, *Astrophys. J.* **420**, 268 (1994).